International Journal of Pure and Applied Mathematics

Volume 36 No. 2 2007, 227-248

NUMERICAL CONFORMAL MAPPING OF DOUBLY CONNECTED REGIONS VIA THE KERZMAN-STEIN KERNEL

Ali H.M. Murid[1], Nurul Akmal Mohamed[2 §]

[1,2]Department of Mathematics
Faculty of Science
University of Technology of Malaysia
81310, UTM Skudai, Johor Darul Ta'zim, MALAYSIA
[1]e-mail: ahmm@mel.fs.utm.my
[2]e-mail: akmalmohdy@yahoo.com.my

Abstract: An integral equation method based on the Kerzman-Stein kernel for conformal mapping of smooth doubly connected regions onto an annulus $A = \{w : \mu < |w| < 1\}$ is presented. The theoretical development is based on the boundary integral equation for conformal mapping of doubly connected regions with Kerzman-Stein kernel derived by Razali and one of the authors [8]. However, the integral equation is not in the form of Fredholm integral equation and no numerical experiments are reported. In this paper, we show that using the boundary relationship satisfied by a function analytic in a doubly connected region, then the previous integral equation can be reduced to a numerically tractable integral equation which however involves the unknown inner radius, μ. For numerical experiments, we discretized the integral equation which leads to an over determined system of non-linear equations. The system obtained is solved simultaneously using Gauss-Newton method and Lavenberg-Marquardt with Fletcher's algorithm for solving the non-linear least squares problems. Numerical implementations on some test regions are also presented.

AMS Subject Classification: 30C30, 30C40, 45G15, 65E05, 65H10
Key Words: conformal mapping, Doubly connected regions, integral equations, Kerzman-Stein kernel, Gauss-Newton method, Lavenberg-Marquardt algorithm, Fletcher's algorithm

Received: February 2, 2007

§Correspondence author

1. Introduction

One approach to solve the Dirichlet problem on a doubly connected region is to conformally transform the given region onto a simpler standard region where it can be solved easily. This method is based on the fact that the Laplace equation is persistence under this mapping. The circular annulus, $A = \{w : \mu < |w| < 1\}$ naturally recommend itself as a standard region for the doubly connected regions. The inner radius (conformal radius), μ is not known in advance and has to be determined in the course of the numerical solution. Several methods have been proposed in the literature for the numerical evaluation for conformal mapping of simply and doubly connected regions. For a recent survey of methods for numerical conformal mapping, see Wegmann [12]. Generally, these methods fall into three types: expansion, iterative and integral equation methods. Common expansion methods are the Bergman and the Szegö kernels method, and the Ritz variational methods. The integral equation and iterative methods are more preferable and effective for numerical conformal mapping. An iterative method by Wegmann [11] consider the conformal mapping from an annulus, $A = \{w : \mu < |w| < 1\}$ onto a given doubly connected region. The method is based on a certain Riemann-Hilbert problem. In view of its quadratic convergence and its $\mathrm{O}(n \log n)$ operations count per iteration step, Wegmann's method is almost certainly the fastest yet devised for this problem. The classical integral equation method of Symm [10] is well-known for computing the conformal maps of doubly connected regions by means of the singular Fredholm integral equations of the first kind. Some Fredholm integral equations of the second kind for conformal mapping of doubly connected regions are of Warschawski and Gerschgorin as discussed in e.g., [4]. All these integral equations are extensions of those maps for simply connected regions. However, there is a recently derived integral equation for conformal mapping of simply connected regions which has no analogue for the doubly connected case. This is the Kerzman-Stein integral equation (briefly KST integral equation) as derived in [4], [5]. An effort for such extension has been given by Murid and Razali [10]. However, the integral equation is not in the form of Fredholm integral equation and no numerical experiment is reported.

In this paper, we show that the integral equation can be reduced to a numerically tractable integral equation which involved the unknown inner radius, μ. For numerical experiments, we discretized the integral equation and imposed the uniqueness condition which leads to an over determined system of non-linear equations. The system obtained is solved using the long accepted method for non-linear least squares problems, called the Gauss-Newton method. However, this classical method only work if a sufficiently close initial estimate p^0 of a solution p^* is known. But, when the Gauss-Newton sequence converges it usually does so rapidly. If the initial estimation is quite far off the final minimum, the modification of the Gauss-Newton named Lavenberg-Marquardt with the Fletcher's algorithm is applied. This method is more robust than the Gauss-Newton algorithm even though it tends to be a bit slower than the Gauss-Newton algorithm. We report on some test regions and give comparisons of our results with results calculated by Amano [2] who developed an interesting charge simulation method for numerical conformal mapping.

2. The Boundary Integral Equation for Conformal Mapping of Doubly Connected Regions with Kerzman-Stein Kernel

Let Ω be the doubly connected domain in the z-plane with boundary $\Gamma = \Gamma_0 \cup \Gamma_1$, where Γ_0 and Γ_1 are the smooth Jordan curves. Let $w = f(z)$ be the analytic function which maps conformally Ω onto the circular annulus $A = \{w : \mu < |w| < 1\}$ so that Γ_0 and Γ_1 correspond respectively to $|w| = 1$ and $|w| = \mu$. The mapping function f is determined up to a factor of modulus 1, that is, up to a rotation of A. The function f could be made unique by prescribing that

$$f(a) > 0\,, \tag{1}$$

or

$$f(z^*) = 1\,, \tag{2}$$

where $a \in \Omega$ and $z^* \in \Gamma_0$ are fixed points.

Suppose the boundary curves Γ_0 and Γ_1 have the following parametric representations:

$$\begin{aligned} \Gamma_0 : z = z_0(t), &\quad 0 \le t \le \beta_0, \\ \Gamma_1 : z = z_1(p), &\quad 0 \le p \le \beta_1. \end{aligned}$$

Hence the boundary values of f can be represented in the form

$$f(z_0(t)) = e^{\mathrm{i}\theta_0(t)}, \quad 0 \le t \le \beta_0, \tag{3}$$

$$f(z_1(p)) = \mu e^{\mathrm{i}\theta_1(p)}, \quad 0 \le p \le \beta_1, \tag{4}$$

where $\theta_0(t)$ and $\theta_1(t)$ are the boundary correspondence functions of Γ_0 and Γ_1 respectively. Denote the unit tangent to Γ at $z(t)$ by $T(z(t)) = z'(t)/|z'(t)|$, then it can be shown that

$$f(z_0(t)) = \frac{1}{\mathrm{i}} T(z_0(t)) \frac{f'(z_0(t))}{|f'(z_0(t))|}, \tag{5}$$

$$f(z_1(p)) = \frac{\mu}{\mathrm{i}} T(z_1(p)) \frac{f'(z_1(p))}{|f'(z_1(p))|}. \tag{6}$$

The boundary relationships (5) and (6) can be combined as

$$f(z) = \frac{|f(z)|}{\mathrm{i}} T(z) \frac{f'(z)}{|f'(z)|}, \quad z \in \Gamma, \tag{7}$$

where $\Gamma = \Gamma_0 \bigcup \Gamma_1$. Recently, Murid and Razali [8] have shown that the mapping function f of doubly connected regions satisfies the integral equation

$$\begin{aligned} \sqrt{f'(z)} \quad &+ \quad \int_\Gamma A(z,w)\sqrt{f'(w)}\,|dw| \\ &= \quad -\mathrm{i}(1-\mu)\overline{T(z)}\left[\frac{1}{2\pi \mathrm{i}}\int_{\Gamma_2} \frac{\sqrt{f'(w)}}{(w-z)f(w)}dw\right]^-, \quad z \in \Gamma, \end{aligned} \tag{8}$$

where the minus sign in the superscript denotes complex conjugation, and

$$A(z,w) = \begin{cases} \overline{H(w,z)} - H(z,w), & w,z \in \Gamma, w \neq z, \\ 0, & w = z \in \Gamma, \end{cases} \tag{9}$$

$$H(w,z) = \frac{1}{2\pi \mathrm{i}} \frac{T(z)}{(z-w)}, \quad w \in \Omega \cup \Gamma, z \in \Gamma, w \neq z, \tag{10}$$

and

$$\Gamma_2 = \begin{cases} -\Gamma_1, & \text{if } z \in \Gamma_0, \\ \Gamma_0, & \text{if } z \in \Gamma_1. \end{cases}$$

The kernel A is known as the Kerzman-Stein kernel [5] and is smooth and skew-Hermitian. The kernel H is the well-known Cauchy kernel. The uniqueness of the solution for the integral equation is guaranteed from the fact that the kernel $A(z,w)$ is skew-hermitian on $\Gamma \times \Gamma$ and therefore has a purely imaginary spectrum. However, no numerical experiments are reported in that paper because the integral equation is not in the form of Fredholm integral equation due to the fact that μ is unknown and evaluation of the right-hand side is yet undetermined.

The single integral equation in (8) can be separated into a system of two integral equations given by

$$\sqrt{f'(z_0)} \quad + \quad \int_\Gamma A(z_0,w)\sqrt{f'(w)}\,|dw|$$

$$= -\mathrm{i}(1 \quad - \quad \mu)\overline{T(z_0)}\left[\frac{1}{2\pi\mathrm{i}}\int_{-\Gamma_1}\frac{\sqrt{f'(w)}}{(w-z_0)f(w)}dw\right]^{-},\ z=z_0\in\Gamma_0, \quad (11)$$

$$\sqrt{f'(z_1)} \quad + \quad \int_\Gamma A(z_1,w)\sqrt{f'(w)}\,|dw|$$
$$= -\mathrm{i}(1 \quad - \quad \mu)\overline{T(z_1)}\left[\frac{1}{2\pi\mathrm{i}}\int_{\Gamma_0}\frac{\sqrt{f'(w)}}{(w-z_1)f(w)}dw\right]^{-},\ z=z_1\in\Gamma_1. \quad (12)$$

Taking the boundary relationship (7) into account, (11) and (12) becomes

$$\sqrt{f'(z_0)} \quad + \quad \int_\Gamma A(z_0,w)\sqrt{f'(w)}\,|dw|$$
$$= -\mathrm{i}(1 \quad - \quad \mu)\overline{T(z_0)}\left[\frac{1}{2\pi\mathrm{i}}\int_{-\Gamma_1}\frac{\sqrt{f'(w)}}{(w-z_0)\left[\frac{\mu}{\mathrm{i}}T(w)\frac{f'(w)}{|f'(w)|}\right]}dw\right]^{-}, \quad z_0\in\Gamma_0,$$

$$\sqrt{f'(z_1)} \quad + \quad \int_\Gamma A(z_1,w)\sqrt{f'(w)}\,|dw|$$
$$= -\mathrm{i}(1 \quad - \quad \mu)\overline{T(z_1)}\left[\frac{1}{2\pi\mathrm{i}}\int_{\Gamma_0}\frac{\sqrt{f'(w)}}{(w-z_1)\left[\frac{1}{\mathrm{i}}T(w)\frac{f'(w)}{|f'(w)|}\right]}dw\right]^{-}, \quad z_1\in\Gamma_1.$$

Using $|f'(w)| = \sqrt{f'(w)}\overline{\sqrt{f'(w)}}$ and $T(w)\,|dw| = dw$, after some mathematical manipulations, the previous two integral equations become

$$\sqrt{f'(z_0)} \quad + \quad \int_\Gamma A(z_0,w)\sqrt{f'(w)}\,|dw|$$
$$= \quad \frac{1}{2\pi\mathrm{i}\mu}(1-\mu)\overline{T(z_0)}\int_{-\Gamma_1}\frac{\sqrt{f'(w)}}{(\overline{w}-\overline{z_0})}\,|dw|, \quad z=z_0\in\Gamma_0, \quad (13)$$

$$\sqrt{f'(z_1)} \quad + \quad \int_\Gamma A(z_1,w)\sqrt{f'(w)}\,|dw|$$
$$= \quad \frac{1}{2\pi\mathrm{i}}(1-\mu)\overline{T(z_1)}\int_{\Gamma_0}\frac{\sqrt{f'(w)}}{(\overline{w}-\overline{z_1})}\,|dw|, \quad z=z_1\in\Gamma_1. \quad (14)$$

Since $\Gamma = \Gamma_0\cup\Gamma_1$, (13) and (14) may be written as

$$\sqrt{f'(z_0)}+\int_{\Gamma_0}A(z_0,w)\sqrt{f'(w)}\,|dw| \quad - \quad \int_{-\Gamma_1}A(z_0,w)\sqrt{f'(w)}\,|dw|$$

$$= \frac{1}{2\pi \mathrm{i}\mu}\int_{-\Gamma_1} \frac{\overline{T(z_0)}}{(\overline{w}-\overline{z_0})}\sqrt{f'(w)}\,|dw| \quad - \quad \frac{1}{2\pi \mathrm{i}}\int_{-\Gamma_1} \frac{\overline{T(z_0)}}{(\overline{w}-\overline{z_0})}\sqrt{f'(w)}\,|dw|,$$

$$\sqrt{f'(z_1)} + \int_{\Gamma_0} A(z_1,w)\sqrt{f'(w)}\,|dw| \quad - \quad \int_{-\Gamma_1} A(z_1,w)\sqrt{f'(w)}\,|dw|$$
$$= \frac{1}{2\pi \mathrm{i}}\int_{\Gamma_0} \frac{\overline{T(z_1)}}{(\overline{w}-\overline{z_1})}\sqrt{f'(w)}\,|dw| \quad - \quad \frac{\mu}{2\pi \mathrm{i}}\int_{\Gamma_0} \frac{\overline{T(z_1)}}{(\overline{w}-\overline{z_1})}\sqrt{f'(w)}\,|dw|.$$

Applying definition in (9) to $A(z_0,w)$ in $\int_{-\Gamma_1}$ of the first equation, and to $A(z_1,w)$ in $\int_{\Gamma_0}$ of the second equation, we obtain

$$\sqrt{f'(z_0)} + \int_{\Gamma_0} A(z_0,w)\sqrt{f'(w)}\,|dw|$$
$$-\int_{-\Gamma_1} \frac{1}{2\pi \mathrm{i}}\left[\frac{\overline{T(z_0)}}{(\overline{w}-\overline{z_0})} - \frac{T(w)}{(w-z_0)}\right]\sqrt{f'(w)}\,|dw|$$
$$= \frac{1}{2\pi \mathrm{i}\mu}\int_{-\Gamma_1} \frac{\overline{T(z_0)}}{(\overline{w}-\overline{z_0})}\sqrt{f'(w)}\,|dw| - \frac{1}{2\pi \mathrm{i}}\int_{-\Gamma_1} \frac{\overline{T(z_0)}}{(\overline{w}-\overline{z_0})}\sqrt{f'(w)}\,|dw|,$$

$$\sqrt{f'(z_1)} \quad + \quad \int_{\Gamma_0} \frac{1}{2\pi \mathrm{i}}\left[\frac{\overline{T(z_1)}}{(\overline{w}-\overline{z_1})} - \frac{T(w)}{(w-z_1)}\right]\sqrt{f'(w)}\,|dw|$$
$$- \quad \int_{-\Gamma_1} A(z_1,w)\sqrt{f'(w)}\,|dw|$$
$$= \quad \frac{1}{2\pi \mathrm{i}}\int_{\Gamma_0} \frac{\overline{T(z_1)}}{(\overline{w}-\overline{z_1})}\sqrt{f'(w)}\,|dw| - \frac{\mu}{2\pi \mathrm{i}}\int_{\Gamma_0} \frac{\overline{T(z_1)}}{(\overline{w}-\overline{z_1})}\sqrt{f'(w)}\,|dw|.$$

After some cancellations, we get

$$\sqrt{f'(z_0)} \quad + \quad \int_{\Gamma_0} A(z_0,w)\sqrt{f'(w)}\,|dw| + \frac{1}{2\pi \mathrm{i}}\int_{-\Gamma_1} \frac{T(w)}{(w-z_0)}\sqrt{f'(w)}\,|dw|$$
$$= \quad \frac{1}{2\pi \mathrm{i}\mu}\int_{-\Gamma_1} \frac{\overline{T(z_0)}}{(\overline{w}-\overline{z_0})}\sqrt{f'(w)}\,|dw|, \quad z = z_0 \in \Gamma_0, \tag{15}$$

$$\sqrt{f'(z_1)} \quad - \quad \frac{1}{2\pi \mathrm{i}}\int_{\Gamma_0} \frac{T(w)}{(w-z_1)}\sqrt{f'(w)}\,|dw| - \int_{-\Gamma_1} A(z_1,w)\sqrt{f'(w)}\,|dw|$$
$$= \quad -\frac{\mu}{2\pi \mathrm{i}}\int_{\Gamma_0} \frac{\overline{T(z_1)}}{(\overline{w}-\overline{z_1})}\sqrt{f'(w)}\,|dw|, \quad z = z_1 \in \Gamma_1. \tag{16}$$

Rearranging (15) and (16) yields

$$\sqrt{f'(z_0)} + \int_{\Gamma_0} A(z_0,w)\sqrt{f'(w)}\,|dw|$$
$$-\int_{-\Gamma_1} \frac{1}{2\pi\mathrm{i}}\left[\frac{\overline{T(z_0)}}{\mu(\overline{w}-\overline{z_0})} - \frac{T(w)}{(w-z_0)}\right]\sqrt{f'(w)}\,|dw| = 0, \quad z = z_0 \in \Gamma_0, \qquad (17)$$

$$\sqrt{f'(z_1)} \;+\; \int_{\Gamma_0} \frac{1}{2\pi\mathrm{i}}\left[\frac{\mu\overline{T(z_1)}}{(\overline{w}-\overline{z_1})} - \frac{T(w)}{(w-z_1)}\right]\sqrt{f'(w)}\,|dw|$$
$$-\; \int_{-\Gamma_1} A(z_1,w)\sqrt{f'(w)}\,|dw| = 0, \quad z = z_1 \in \Gamma_1. \qquad (18)$$

Note that there are three unknown quantities in the integral equations (17) and (18), namely, $\sqrt{f'(z_0)}$, $\sqrt{f'(z_1)}$ and μ. For numerical purposes, another equation involving μ is needed so that the system of integral equations above can be solved simultaneously. This third equation is derived next. Consider equation (3) and (4) which upon differentiation gives

$$\begin{aligned} f'(z_0(t))z_0'(t) &= e^{\mathrm{i}\theta_0(t)}\mathrm{i}\theta_0'(t), \\ f'(z_1(p))z_1'(p) &= \mu e^{\mathrm{i}\theta_1(p)}\mathrm{i}\theta_1'(p). \end{aligned}$$

Taking the modulus for both sides of the equations, we obtain

$$|f'(z_0(t))z_0'(t)| = |e^{\mathrm{i}\theta_0(t)}\mathrm{i}\theta_0'(t)| = |e^{\mathrm{i}\theta_0(t)}||\mathrm{i}||\theta_0'(t)|, \qquad (19)$$
$$|f'(z_1(p))z_1'(p)| = |\mu e^{\mathrm{i}\theta_1(p)}\mathrm{i}\theta_1'(p)| = |\mu||e^{\mathrm{i}\theta_1(p)}||\mathrm{i}||\theta_1'(p)|. \qquad (20)$$

The absolute values of $e^{\mathrm{i}\theta_0(t)}$ and $e^{\mathrm{i}\theta_1(p)}$ are both equal to 1. The boundary correspondence functions $\theta_0(t)$ and $\theta_1(p)$ are increasing monotone functions and thus the derivative of them are never negative which give $|\theta_0'(t)| = \theta_0'(t)$ and $|\theta_1'(p)| = \theta_1'(p)$. μ is the inner radius of the annulus $A = \{w : \mu < |w| < 1\}$ where $0 < \mu < 1$. Thus (19) and (20) can now be written as

$$|f'(z_0(t))z_0'(t)| = \theta_0'(t), \qquad (21)$$
$$|f'(z_1(p))z_1'(p)| = \mu\theta_1'(p). \qquad (22)$$

Upon integrating (21) and (22) respectively with respect to t and p from 0 to 2π gives

$$\int_0^{2\pi} |f'(z_0(t))z_0'(t)|dt = \int_0^{2\pi} \theta_0'(t)dt = \theta_0'(t)|_0^{2\pi} = 2\pi, \qquad (23)$$
$$\int_0^{2\pi} |f'(z_1(p))z_1'(p)|dp = \mu\int_0^{2\pi} \theta_1'(p)dp = \mu\theta_1'(p)|_0^{2\pi} = \mu 2\pi. \qquad (24)$$

Subtracting (23) from (24) multiplied by μ, we obtain

$$\mu \int_0^{2\pi} |f'(z_0(t))z_0'(t)|\, dt - \int_0^{2\pi} |f'(z_1(p))z_1'(p)|\, dp = 0, \tag{25}$$

which is the required third equation.

Defining

$$\begin{aligned} g(z) &= \sqrt{f'(z)}, \quad B(z,w) = \frac{1}{2\pi \mathrm{i}} \left[\frac{\overline{T(z)}}{\mu(\overline{w}-\overline{z})} - \frac{T(w)}{(w-z)} \right], \\ D(z,w) &= \frac{1}{2\pi \mathrm{i}} \left[\frac{\mu\overline{T(z)}}{(\overline{w}-\overline{z})} - \frac{T(w)}{(w-z)} \right], \end{aligned}$$

(17) and (18) can be written briefly as

$$g(z_0) + \int_{\Gamma_0} A(z_0,w)g(w)\,|dw| - \int_{-\Gamma_1} B(z_0,w)g(w)\,|dw| = 0,\ z_0 \in \Gamma_0, \tag{26}$$

$$g(z_1) + \int_{\Gamma_0} D(z_1,w)g(w)\,|dw| - \int_{-\Gamma_1} A(z_1,w)g(w)\,|dw| = 0,\ z_1 \in \Gamma_1. \tag{27}$$

Note that the system of integral equations in (26), (27) and (25) is homogeneous and does not have a unique solution; if $\{\mu, \sqrt{f'(z)}\}$ is the solution set, then so is $\{\mu, \kappa\sqrt{f'(z)}\}$ for arbitrary complex number κ.

3. Numerical Implementation

Using parametric representation $z_0(t)$ of Γ_0 for $t : 0 \le t \le \beta_0$ and $z_1(p)$ of Γ_1 for $p : 0 \le p \le \beta_1$, (26) and (27) become

$$\begin{aligned} g(z_0(t)) &+ \int_0^{\beta_0} A(z_0(t), z_0(s))g(z_0(s))|z_0'(s)|\, ds \\ &- \int_0^{\beta_1} B(z_0(t), z_1(q))g(z_1(q))|z_1'(q)|\, dq = 0, \quad z_0(t) \in \Gamma_0, \end{aligned} \tag{28}$$

$$\begin{aligned} g(z_1(p)) &+ \int_0^{\beta_0} D(z_1(p), z_0(s))g(z_0(s))|z_0'(s)|\, ds \\ &- \int_0^{\beta_1} A(z_1(p), z_1(q))g(z_1(q))|z_1'(q)|\, dq = 0, \quad z_1(p) \in \Gamma_1. \end{aligned} \tag{29}$$

Multiply (28) and (29) respectively by $|z_0'(t)|^{1/2}$ and $|z_1'(p)|^{1/2}$ gives

$$\begin{aligned} &|z_0'(t)|^{1/2} g(z_0(t)) \\ &\qquad + \int_0^{\beta_0} |z_0'(t)|^{1/2}|z_0'(s)|^{1/2} A(z_0(t), z_0(s)) g(z_0(s)) |z_0'(s)|^{1/2}\, ds \\ &\qquad - \int_0^{\beta_1} |z_0'(t)|^{1/2}|z_1'(q)|^{1/2} B(z_0(t), z_1(q)) g(z_1(q)) |z_1'(q)|^{1/2}\, dq = 0, \end{aligned} \tag{30}$$

$$\begin{aligned} &|z_1'(p)|^{1/2} g(z_1(p)) \\ &\qquad + \int_0^{\beta_0} |z_1'(p)|^{1/2}|z_0'(s)|^{1/2} D(z_1(p), z_0(s)) g(z_0(s)) |z_0'(s)|^{1/2}\, ds \\ &\qquad - \int_0^{\beta_1} |z_1'(p)|^{1/2}|z_1'(q)|^{1/2} A(z_1(p), z_1(q)) g(z_1(q)) |z_1'(q)|^{1/2}\, dq = 0. \end{aligned} \tag{31}$$

Defining

$$\begin{aligned} \phi_0(t) &= |z_0'(t)|^{1/2} g(z_0(t)), \quad \phi_1(p) = |z_1'(p)|^{1/2} g(z_1(p)), \\ K_{00}(t,s) &= |z_0'(t)|^{1/2}|z_0'(s)|^{1/2} A(z_0(t), z_0(s)), \\ K_{01}(t,q) &= |z_0'(t)|^{1/2}|z_1'(q)|^{1/2} B(z_0((t), z_1(q)), \\ K_{10}(p,s) &= |z_1'(p)|^{1/2}|z_0'(s)|^{1/2} D(z_1(p), z_0(s)), \\ K_{11}(p,q) &= |z_1'(p)|^{1/2}|z_1'(q)|^{1/2} A(z_1(p), z_1(q)), \end{aligned}$$

and so (30) and (31) become

$$\phi_0(t) + \int_0^{\beta_0} K_{00}(t,s)\ \phi_0(s)\ ds - \int_0^{\beta_1} K_{01}(t,q)\ \phi_1(q)\ dq = 0,\ z_0(t) \in \Gamma_0, \tag{32}$$

$$\phi_1(p) + \int_0^{\beta_0} K_{10}(p,s)\ \phi_0(s)\ ds - \int_0^{\beta_1} K_{11}(p,q)\ \phi_1(q)\ dq = 0,\ z_1(p) \in \Gamma_1. \tag{33}$$

Note that the kernel $K_{00}(t,s)$ and $K_{11}(p,q)$ preserve the skew-Hermitian properties. Applying the same procedure to equation (25), we get

$$\mu \int_0^{2\pi} |\phi_0(t)|^{\ 2}\ dt - \int_0^{2\pi} |\phi_1(p)|^{\ 2}\ dp = 0. \tag{34}$$

which is the third equation involving μ that can be solve simultaneously with integral equations (32) and (33).

Since the functions ϕ and K are β -periodic, an appealing procedure for solving (32), (33) and (34) numerically is using the Nyström's method with the trapezoidal rule [3]. The trapezoidal rule is the most accurate method for integrating periodic functions numerically. Choosing n equidistant collocation points $t_i = (i-1)\beta_0/n$, $1 \le i \le n$ and m equidistant collocation points $p_\imath = (\imath - 1)\beta_1/m$, $1 \le \imath \le m$ before then applying the trapezoidal rule for Nyström's method to discretize (32), (33) and (34), we obtain

$$\phi_0(t_i) + \frac{\beta_0}{n}\sum_{j=1}^{n} K_{00}(t_i,t_j)\,\phi_0(t_j) - \frac{\beta_1}{m}\sum_{\jmath=1}^{m} K_{01}(t_i,p_\jmath)\,\phi_1(p_\jmath) = 0, \tag{35}$$

$$\phi_1(p_\imath) + \frac{\beta_0}{n}\sum_{j=1}^{n} K_{10}(p_\imath,t_j)\,\phi_0(t_j) - \frac{\beta_1}{m}\sum_{\jmath=1}^{m} K_{11}(p_\imath,p_\jmath)\phi_1(p_\jmath) = 0, \tag{36}$$

$$\mu\frac{\beta_0}{n}\sum_{i=1}^{n} |\phi_0(t_i)|^2 - \frac{\beta_1}{m}\sum_{\imath=1}^{m} |\phi_1(p_\imath)|^2 = 0. \tag{37}$$

Note that in the third equation (37),

$$|\phi_0| = \sqrt{(\operatorname{Re}\phi_0)^2 + (\operatorname{Im}\phi_0)^2}, \quad |\phi_1| = \sqrt{(\operatorname{Re}\phi_1)^2 + (\operatorname{Im}\phi_1)^2}.$$

Equations (35), (36) and (37) lead to a system of $(n+m+1)$ nonlinear complex equations in n unknowns $\phi_0(t_i)$, m unknowns $\phi_1(p_\imath)$ and μ. By defining the matrices

$$\begin{aligned} B_{ij} &= \frac{\beta_0}{n}K_{00}(t_i,t_j), \quad C_{i\jmath} = \frac{\beta_1}{m}K_{01}(t_i,p_\jmath),\\ E_{\imath j} &= \frac{\beta_0}{n}K_{10}(p_\imath,t_j), \quad D_{\imath\jmath} = \frac{\beta_1}{m}K_{11}(p_\imath,p_\jmath),\\ x_{0i} &= \phi_0(t_i), \quad x_{1\imath} = \phi_1(p_\imath), \end{aligned}$$

the system of equations in (35) and (36) can be written as $n+m$ by $n+m$ system

$$[I_{nn} + B_{nn}]\,\mathbf{x}_{0n} - C_{nm}\mathbf{x}_{1m} = \mathbf{0}_{0n}, \tag{38}$$

$$E_{mn}\mathbf{x}_{0n} + [\,I_{mm} - D_{mm}]\,\mathbf{x}_{1m} = \mathbf{0}_{1m}. \tag{39}$$

In addition, equation (37) becomes

$$\mu\frac{\beta_0}{n}\sum_{i=1}^{n} ((\operatorname{Re}\ x_{0i})^2 + (\operatorname{Im}\ x_{0i})^2) - \frac{\beta_1}{m}\sum_{\imath=1}^{m}((\operatorname{Re}\ x_{1\imath})^2 + (\operatorname{Im}\ x_{1\imath})^2) = 0. \tag{40}$$

The result in matrix form for system of equations (38) and (39) is

$$\begin{pmatrix} I_{nn}+B_{nn} & \vdots & -C_{nm} \\ \cdots & \cdots & \cdots \\ E_{mn} & \vdots & I_{mm}-D_{mm} \end{pmatrix} \begin{pmatrix} \mathbf{x}_{0n} \\ \cdots \\ \mathbf{x}_{1m} \end{pmatrix} = \begin{pmatrix} \mathbf{0}_{0n} \\ \cdots \\ \mathbf{0}_{1m} \end{pmatrix}.$$

Defining

$$A = \begin{pmatrix} I_{nn}+B_{nn} & \vdots & -C_{nm} \\ \cdots & \cdots & \cdots \\ E_{mn} & \vdots & I_{mm}-D_{mm} \end{pmatrix},$$

$$\mathbf{x}= \begin{pmatrix} \mathbf{x}_{0n} \\ \cdots \\ \mathbf{x}_{1m} \end{pmatrix} \quad \text{and} \quad \mathbf{0} = \begin{pmatrix} \mathbf{0}_{0n} \\ \cdots \\ \mathbf{0}_{1m} \end{pmatrix},$$

the $(n+m)\times(n+m)$ complex system can be written briefly as $A\mathbf{x} = \mathbf{0}$. Separating A and $\mathbf{x}$ in terms of the real and imaginary parts, the system can be written as

$$\mathrm{Re}\ A\ \mathrm{Re}\ \mathbf{x} - \mathrm{Im}\ A\ \mathrm{Im}\ \mathbf{x} + \mathrm{i}\,(\mathrm{Re}\ A\ \mathrm{Im}\ \mathbf{x} + \mathrm{Im}\ A\ \mathrm{Re}\ \mathbf{x}) = \mathbf{0} + \mathbf{0}\mathrm{i}.$$

Thus, the single $(n+m)\times(n+m)$ complex linear system above is equivalent to the $2(n+m)\times 2(n+m)$ real system involving the Re and Im of the unknown functions, i.e.,

$$\begin{pmatrix} \mathrm{Re}\, A & \vdots & -\mathrm{Im}\, A \\ \cdots & \cdots & \cdots \\ \mathrm{Im}\, A & \vdots & \mathrm{Re}\, A \end{pmatrix} \begin{pmatrix} \mathrm{Re}\,\mathbf{x} \\ \cdots \\ \mathrm{Im}\,\mathbf{x} \end{pmatrix} = \begin{pmatrix} \mathbf{0} \\ \cdots \\ \mathbf{0} \end{pmatrix}. \tag{41}$$

Therefore, the linear system above can be solved simultaneously with the nonlinear equation (40) which also involves the Re and Im parts of the unknown functions. Since the system of integral equations (32), (33) and (34) has no unique solution, the system of equations (41) and (40) also in general has no unique solution. For uniqueness, we turn to the conditions (1) or (2).

Since we are dealing with boundary values, the second condition looks more appropriate for our numerical purpose. However, it leads to a difficulty as discussed next. We first assume that $z_0(t_1) = z_0(0)$ is to be mapped onto 1 under the mapping function f. For the test regions that we have chosen in Section 4, the unit tangent vector $T(z_0(t_1))$ is equal to i. For $z = z_0(t_1)$, the boundary relationship (7) yields

$$1 = \frac{f'(z_0(t_1))}{|f'(z_0(t_1))|},$$

or

$$f'(z_0(t_1)) = |f'(z_0(t_1))|. \tag{42}$$

Making use of (21) and (42) give

$$\mathrm{Re}\, x_{01} + \mathrm{i}\mathrm{Im}\, x_{01} = \phi_0(t_1) = \sqrt{f'(z_0(t_1))|z_0'(t_1)|} = \sqrt{\theta_0'(t_1)}, \tag{43}$$

which yields immediately the conditions

$$\begin{cases} \mathrm{Re}\, x_{01} = \sqrt{\theta_0'(t_1)}, \\ \mathrm{Im}\, x_{01} = 0. \end{cases} \tag{44}$$

But $\theta_0'(t_1)$ is unknown in advance. By knowing only the imaginary part of x_{01} without its real part will not yield a unique solution of equations (40) and (41). A different strategy for getting the required uniqueness condition is described next.

As is well known that the mapping function, f exists up to a rotation of the annulus, that is up to a factor of modulus 1 [4]. For a given f, suppose f is made unique by prescribing $f(z_0(0)) = 1$. Then, the function F such that

$$F(z) = e^{\mathrm{i}\alpha} f(z), \tag{45}$$

for arbitrary $\alpha \in \Re$, also maps a doubly connected region onto an annulus.

Differentiating (45) gives

$$F'(z) = e^{\mathrm{i}\alpha} f'(z) \quad \text{or} \quad \sqrt{F'(z)} = \sqrt{e^{\mathrm{i}\alpha} f'(z)}. \tag{46}$$

Note that if $\{\mu, \sqrt{F'(z)}\}$ is the solution set of (32), and (33), then so is $\{\mu, \kappa\sqrt{F'(z)}\}$ or $\{\mu, \kappa\sqrt{e^{\mathrm{i}\alpha} f'(z)}\}$, where κ is any complex number.

Suppose

$$F^*(z) = re^{\mathrm{i}\alpha} f(z), \quad r, \alpha \in \Re, \tag{47}$$

is a mapping function that maps a doubly connected region onto an annulus $A^* = \{w : r\mu < |w| < r\}$ and the $\mathrm{Arg}(F^*(z))$ and $\mathrm{Arg}(f(z))$ differ by α.

Differentiating (47), gives

$$F^{*\prime}(z) = re^{\mathrm{i}\alpha} f'(z) \quad \text{or} \quad \sqrt{F^{*\prime}(z)} = \sqrt{re^{\mathrm{i}\alpha} f'(z)}\,.$$

Since $\sqrt{r} \in \Re \subseteq C$, then $\{\mu, \sqrt{F^{*\prime}(z)}\}$ is also the solution set of our integral equations (32) and (33). Note that $F^{*\prime}$ also satisfies (25).

The boundary relationship (7) implies

$$e^{\mathrm{i}\alpha} f(z) = \frac{|e^{\mathrm{i}\alpha} f(z)|}{\mathrm{i}} T(z) \frac{re^{\mathrm{i}\alpha} f'(z)}{|re^{\mathrm{i}\alpha} f'(z)|}, \quad z \in \Gamma. \tag{48}$$

Since $e^{\mathrm{i}\alpha} f(z) = F(z)$ and $re^{\mathrm{i}\alpha} f(z) = F^*(z)$, (48) can also be written as

$$F(z) = \frac{|F(z)|}{\mathrm{i}} T(z) \frac{F^{*\prime}(z)}{|F^{*\prime}(z)|}, \quad z \in \Gamma, \tag{49}$$

where $|F(z)|$ is either 1 or μ. The idea now is to solve for the unique solution $\sqrt{F^{*\prime}(z)}$ from the system of integral equations (32), (33) and (25) with a prescribing value of $F^{*\prime}(z_0(0))$. If $F^{*\prime}(z_0(0)) = B^*$, then

$$\operatorname{Re} x_{01} + \mathrm{i} \operatorname{Im} x_{01} = \phi_0(t_1) = \sqrt{F^{*\prime}(z_0(t_1))|z_0'(t_1)|} = \sqrt{B^* \, |z_0'(t_1)|} \, ,$$

or

$$\begin{cases} \operatorname{Re} x_{01} = \operatorname{Re} \sqrt{B^* \, |z_0'(t_1)|}, \\ \operatorname{Im} x_{01} = \operatorname{Im} \sqrt{B^* \, |z_0'(t_1)|} \, . \end{cases} \tag{50}$$

The boundary values of $F(z)$ are then computed according to equation (49). By means of equation (45), we then have

$$f(z) = e^{-\mathrm{i}\alpha} F(z), \quad z \in \Gamma.$$

It remains to determine α. Observe that

$$F^*(z_0(t)) = re^{\mathrm{i}\alpha} f(z_0(t)) = re^{\mathrm{i}\alpha} e^{\mathrm{i}\theta_0(t)}. \tag{51}$$

Differentiating (51), we obtain

$$F^{*\prime}(z_0(t)) z_0'(t) = re^{\mathrm{i}\alpha} \mathrm{i}\theta_0'(t) e^{\mathrm{i}\theta_0(t)}.$$

Substituting $t_1 = 0$, gives

$$F^{*\prime}(z_0(0)) z_0'(0) = re^{\mathrm{i}\alpha} \mathrm{i}\theta_0'(0).$$

Since $F^{*\prime}(z_0(0)) = B^*$, α is then calculated by the formula

$$\alpha = \operatorname{Arg}[-\mathrm{i} z_0'(0) B^*].$$

The system of equations (40), (41) and (50) is an over determined system of nonlinear equations involving $2(n+m)+3$ equations in $2(n+m)+1$ unknowns. Method for solving system having unequal number of equations and unknowns are best dealt with as problems in optimization [13]. The solution of this system of equations will coincide with the minimizer of a function which is produced by taking the sum of squares of the left-hand sides of the over determined system of the nonlinear equations (the right-hand sides of the equations being zero). We use Gauss-Newton algorithm to solve this nonlinear least square problem which is a modification of Newton's method that does not use second derivatives. Some discussion on this method is found in [1], [7], [13], [15].

Our nonlinear least squares problem consists in finding the vector $\mathbf{p}$ for which the function $S : R^{2(n+m)+3} \to R^1$ defined by the sum

$$S(\mathbf{p}) = \mathbf{f}^T\mathbf{f} = \sum_{i=1}^{2(n+m)+3} (f_i(\mathbf{p}))^2$$

is minimal. Here, $\mathbf{p}$ stands for the $2(n+m)+1$-vector ($\operatorname{Re} x_{01}$, $\operatorname{Re} x_{02}$, ..., $\operatorname{Re} x_{0n}$, $\operatorname{Re} x_{11}$, $\operatorname{Re} x_{12}$, ..., $\operatorname{Re} x_{1m}$, $\operatorname{Im} x_{01}$, $\operatorname{Im} x_{02}$, ..., $\operatorname{Im} x_{0n}$, $\operatorname{Im} x_{11}$, $\operatorname{Im} x_{12}$, ..., $\operatorname{Im} x_{1m}$, μ), and $\mathbf{f} = (f_1, f_2, ..., f_{2(n+m)+3})$. The Gauss-Newton algorithm is an iterative procedure and we have to provide an initial guess for the vector $\mathbf{p}$, denoted as $\mathbf{p}^0$. This initial approximation, which, if at all possible, should be a well-informed guess and generate a sequence of approximations $\mathbf{p}^1$, $\mathbf{p}^2$, $\mathbf{p}^3$, ... based on the formula

$$\mathbf{p}^{k+1} = \mathbf{p}^k - ((J_{\mathbf{f}}(\mathbf{p}^k))^{\mathrm{T}} J_{\mathbf{f}}(\mathbf{p}^k))^{-1}(J_{\mathbf{f}}(\mathbf{p}^k))^{\mathrm{T}}\mathbf{f}(\mathbf{p}^k), \tag{52}$$

where $J_{\mathbf{f}}(\mathbf{p})$ denotes the Jacobian of $\mathbf{f}$ at $\mathbf{p}$ (note that $J_{\mathbf{f}}(\mathbf{p})$ is not square but $(2(n+m)+3) \times (2(n+m)+1)$ matrix). It is reasonable to use the convergence criterion

$$||\mathbf{p}^{(k+1)} - \mathbf{p}^{(k)}|| \le \varepsilon, \quad \text{and} \quad |S^{(k+1)} - S^{(k)}| \le \varepsilon,$$

where ε is predefined tolerances expressing the desired level of accuracy which has been chosen as 1×10^{-13} and $||\ ||$ is the vector norm.

The strategy for getting the initial estimation is based on (3) and (4) where upon differentiating and squaring the two equations, we obtain

$$\begin{aligned} \phi_0(t) = & \sqrt{f(z_0(t))z_0'(t)} & = \sqrt{\mathrm{i}\theta_0'(t)e^{\mathrm{i}\theta_0(t)}}, \\ \phi_1(t) = & \sqrt{f(z_1(p))z_1'(p)} & = \sqrt{\mu\mathrm{i}\theta_1'(p)e^{\mathrm{i}\theta_1(p)}}. \end{aligned}$$

For initial estimation, we assume $\theta_0(t) = t$ and $\theta_1(p) = p$ which implies $\theta_0'(t) = \theta_1'(p) = 1$. The inner radius , μ is given the initial estimation 0.5 for all regions, except for circular frame which is approximated by ρ. This initial guess is applied for the lowest number of n and m of our experiments. In all our numerical experiments, we have chosen the number of collocation points on Γ_0 and Γ_1 being equal, i.e. $n = m$. The information from the solution for lower n is then exploited to calculate the starting vector $\mathbf{p}^0$ related to $2n$ number of collocation points.

The numerical implementations on some test regions show that the Gauss-Newton method is successful for all test regions except for the frame of Cassini's oval. This problem occurs since our initial estimation is quite far off the final minimum.

It has been discussed in the literature [13] that the Gauss-Newton method is too naive for the solution of the least squares problems. Most of the effective methods for solving the least squares problem which are currently in use are, however, modifications of the Gauss-Newton method. In this paper, we have applied one of the modification of the Gauss-Newton named Lavenberg-Marquardt with the Fletcher's algorithm [13]. This method is more robust than the Gauss-Newton algorithm and is reasonably efficient and reliable on the frame of Cassini's oval. The Lavenberg-Marquardt algorithm combines the Gauss-Newton method and steepest descent method. Whereas Gauss-Newton method converges quadratically in a neighborhood of the root, the steepest descent method converges only linearly. However, the steepest descent method converges to one of the local minima starting from almost arbitrary starting values while the Gauss-Newton method requires a good initial approximation.

The key to the Lavenberg-Marquardt algorithm is to replace (52) by

$$\mathbf{p}^{k+1} = \mathbf{p}^k - H(\mathbf{p}^k)\mathbf{f}(\mathbf{p}^k), \quad \lambda^k \geq 0\,,$$

where $H(\mathbf{p}^k) = ((J_{\mathbf{f}}(\mathbf{p}^k))^{\mathrm{T}} J_{\mathbf{f}}(\mathbf{p}^k) + \lambda^k)^{-1}(J_{\mathbf{f}}(\mathbf{p}^k))^{\mathrm{T}}$.

For $\lambda^k = 0$, it yields the Gauss-Newton method, whereas as λ^k increases, the direction specified by $H(\mathbf{p}^k)$ tends to that of the steepest descent method. Thus, in this algorithm, we start with a large value of λ^k and go on reducing it as the solution is approached, so as to switch from the method of steepest descent to the Newton's method. This Lavenberg-Marquardt with Fletcher's algorithm is applied in our numerical implementation. The difference between the methods of original Lavenberg-Marquardt algorithm and with Fletcher's algorithm lies in the used of methods which are used to determined suitable values for the λ^k.

Using (45), the boundary correspondence function $\theta(t)$ is defined as

$$\theta(t) = \mathrm{Arg}(e^{-\mathrm{i}\alpha} F(z(t))) \quad \text{or} \quad \theta(t) = -\alpha + \mathrm{Arg}(F(z(t))).$$

Solving this equation for the unknown function $\mathrm{Re}\, x_{0i} + \mathrm{i}\mathrm{Im}\, x_{0i} = \phi_0(t_i) = \sqrt{F^{*\prime}(z_0(t_i))|z_0{}'(t_i)|}$, $\mathrm{Re}\, x_{1\imath} + \mathrm{i}\mathrm{Im}\, x_{1\imath} = \phi_1(p_\imath) = \sqrt{F^{*\prime}(z_1(p_\imath))|z_1'(p_\imath)|}$ and μ and by using the boundary relationship (49) allows us the compute the indicated boundary correspondence functions $\theta_0(t)$ and $\theta_1(p)$ by the formula

$$\theta_0(t) = -\alpha + \mathrm{Arg}(-\mathrm{i}\, z_0'(t)\, \phi_0^2(t)), \quad (53)$$

$$\theta_1(p) = -\alpha + \mathrm{Arg}(-\mathrm{i}\, z_1'(p)\phi_1^2(p)). \quad (54)$$

4. Examples and Numerical Results

For our numerical experiments, we have used four test regions whose exact boundary correspondence functions are known. The test regions are frame of Limacon, Cassini's oval, elliptic frame and circular frame. The results for the sub-norm error of the boundary correspondence functions $\theta_0(t)$ and $\theta_1(p)$ and the value μ is shown in Tables 1 to 4. All the computations are done using *Mathematica* package [14] in single precision (16 digit machine precision). The numerical computations for the elliptic frame and frame of Cassini's oval are compared with those obtained by Amano [2], though his distribution is different from ours. The notations E_M and E_A that are used by Amano are defined as follows:

$$E_M = \max\{\max_i ||f(z_0(t_i)| - 1|, \max_i ||f(z_1(t_i)| - \mu|\},$$

$$E_A = \max\{\|\theta_0(t) - \theta_{0n}(t)\|_\infty, \|\theta_1(p) - \theta_{1m}(p)\|_\infty\}.$$

Example 1. (Frame of Limacon, see Figure 1) Consider a pair of Limacons [6],

$$\Gamma_0 : \{z(t) = a_0 \cos t + b_0 \cos 2t + i(a_0 \sin t + b_0 \sin 2t), a_0 > 0, b_0 > 0\},$$
$$\Gamma_1 : \{z(t) = a_1 \cos t + b_1 \cos 2t + i(a_1 \sin t + b_1 \sin 2t), a_1 > 0, b_1 > 0\},$$

with $a_1 = 5, a_0 = 10, b_0 = 3$, and $b_1 = b_0/4$, where $t : 0 \le t \le 2\pi$. The values of a_0, a_1, b_0, and b_1 are chosen so that $b_1/b_0 = a_1/a_0$, which ensures that the function

$$f(z) = \frac{\sqrt{a_0^2 + 4b_0 z} - a_0}{2b_0},$$

which maps Γ_0 onto the unit circle also maps Γ_1 onto a circle of radius $\mu = 1/M = a_1/a_0$. See Table 1 for results.

Example 2. (Frame of Cassini's Oval, see Figure 2) If Ω is the domain bounded by two Cassini's oval, then the complex parametric equation of its

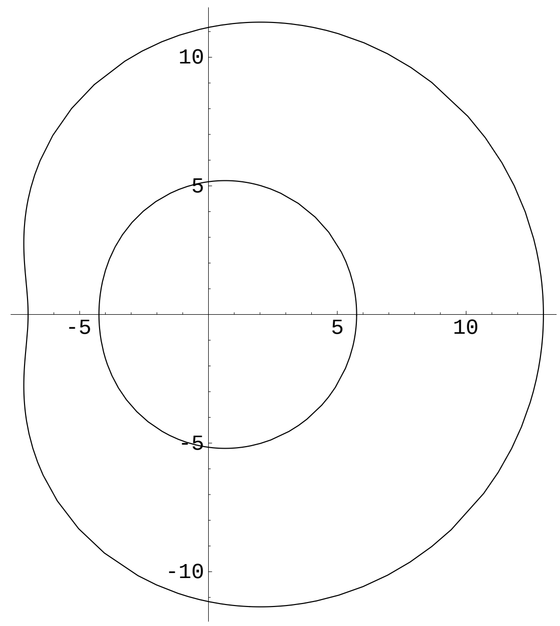

Figure 1: Frame of limacon

$n = m$	$\\|\theta_0(t) - \theta_{0n}(t)\\|_\infty$	$\\|\theta_1(p) - \theta_{1m}(p)\\|_\infty$	$\\|\mu - \mu_m\\|_\infty$
16	9.7(−06)	5.1(−06)	2.8(−05)
32	4.2(−10)	3.1(−10)	2.1(−10)
64	1.3(−15)	1.8(−15)	1.1(−16)

Table 1: Error norm (frame of limacon)

boundary is given by [2],

$$\Gamma_0 : \{z(t) = \sqrt{b_0^2 \cos 2t + \sqrt{a_0^4 - b_0^4 \sin^2 2t}} e^{it}, a_0 > 0, b_0 > 0\},$$

$$\Gamma_1 : \{z(t) = \sqrt{b_1^2 \cos 2t + \sqrt{a_1^4 - b_1^4 \sin^2 2t}} e^{it}, a_1 > 0, b_1 > 0\},$$

where $t : 0 \leq t \leq 2\pi$, such that

$$\Omega \ : |z^2 - b_0^2| < a_0^2, \quad |z^2 - b_1^2| > a_1^2 \,.$$

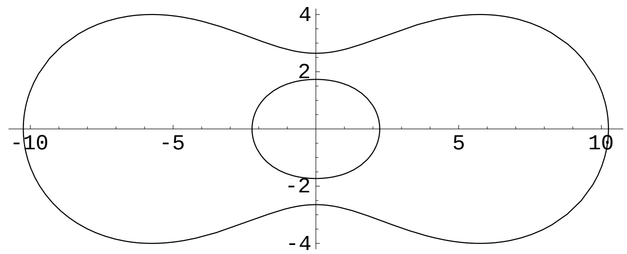

Figure 2: Frame of Cassini's oval

$n=m$	$\|\theta_0(t)-\theta_{0n}(t)\|_\infty$	$\|\theta_1(p)-\theta_{1m}(p)\|_\infty$	$\|\mu-\mu_m\|_\infty$
16	6.4(−03)	2.5(−03)	2.1(−03)
32	6.9(−05)	2.7(−05)	2.1(−05)
64	1.1(−08)	3.7(−09)	3.9(−09)

Table 2: Error norm (frame of Cassini's oval) using our method

$n=m$	E_A	E_M
16	9.7(−03)	9.1(−03)
32	3.8(−04)	3.4(−04)
64	5.0(−07)	6.9(−07)

Table 3: Error norm (frame of Cassini's oval) using Amano's method

The analytic solution is known when $(a_0^4-b_0^4)/b_0^2=(a_1^4-b_1^4)/b_1^2$ which is given by

$$f(z)=\frac{a_0 z}{\sqrt{b_0^2z^2+a_0^4-b_0^4}},\quad \text{and}\quad \mu=\frac{a_1}{a_0}.$$

We choose $a_0=2\sqrt{14}$, $b_0=7$, $a_1=2$ and $b_1=1$ so that the exact mapping function is satisfied. Table 2 shows the results. The results obtained using Amano's method [2] are also shown in Table 3 for comparison.

Example 3. (Circular Frame, see Figure 3) Consider a pair of circles [9]

$$\Gamma_0 : \{z(t)=e^{it}\},$$
$$\Gamma_1 : \{z(t)=c+\rho e^{it}\},\quad t:0\le t\le 2\pi,$$

such that the domain bounded by Γ_0 and Γ_1 is the domain between a unit circle and a circle center at c with radius ρ. The exact mapping function is given by

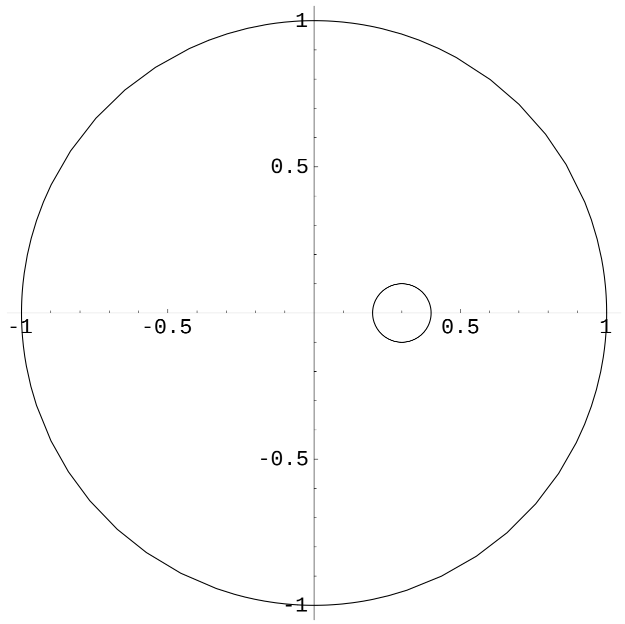

Figure 3: Circular frame

$n = m$	$\\|\theta_0(t) - \theta_{0n}(t)\\|_\infty$	$\\|\theta_1(p) - \theta_{1m}(p)\\|_\infty$	$\\|\mu - \mu_m\\|_\infty$
8	9.8(−11)	4.6(−09)	1.4(−06)
16	8.9(−16)	7.1(−15)	9.5(−11)

Table 4: Error norm (circular frame)

$f(z) = (z - \lambda)/(\lambda z - 1)$, with

$$\lambda = \frac{2c}{1 + (c^2 - \rho^2) + \sqrt{(1 - (c - \rho)^2)(1 - (c + \rho)^2)}},$$

which maps Γ_0 onto the unit circle and Γ_1 onto a circle of radius

$$\mu = 1/M = \frac{2\rho}{1 + (c^2 - \rho^2) + \sqrt{(1 - (c - \rho)^2)(1 - (c + \rho)^2)}}.$$

See Table 4 for the numerical result.

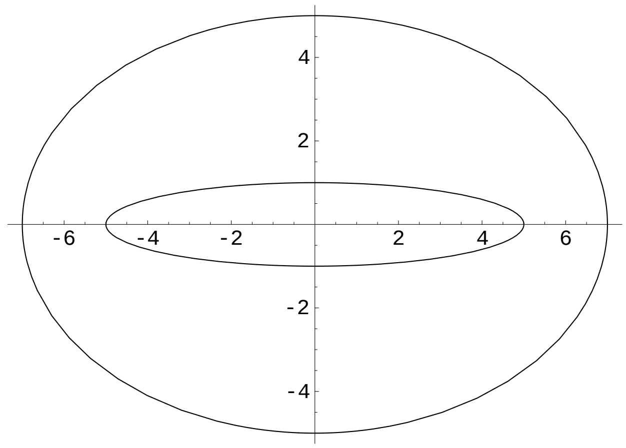

Figure 4: Elliptic frame

$n = m$	$\|\theta_0(t) - \theta_{0n}(t)\|_\infty$	$\|\theta_1(p) - \theta_{1m}(p)\|_\infty$	$\|\mu - \mu_m\|_\infty$
16	4.0(−04)	3.2(−04)	3.7(−05)
32	5.1(−06)	1.0(−05)	3.7(−06)
64	2.7(−09)	5.9(−09)	2.2(−09)
128	3.6(−15)	5.8(−15)	1.8(−15)

Table 5: Error norm (elliptic frame) using our method

Example 4. (Elliptic Frame, see Figure 4) Elliptic frame is the domain bounded by two Jordan curves, Γ_0 and Γ_1 such that

$$\Omega : \frac{x^2}{a_0^2} + \frac{y^2}{b_0^2} < 1, \quad \frac{x^2}{a_1^2} + \frac{y^2}{b_1^2} > 1,$$

with the complex parametric of its boundary is given by [2],

$$\Gamma_0 : \{z(t) = a_0 \cos t + ib_0 \sin t, a_0 > 0, b_0 > 0\},$$
$$\Gamma_1 : \{z(t) = a_1 \cos t + ib_1 \sin t, a_1 > 0, b_1 > 0\}.$$

The analytic solution is known when the two ellipses Γ_0 and Γ_1 are confocal such that $a_0^2 - b_0^2 = a_1^2 - b_1^2$ which is given by

$$f(z) = \frac{z + \sqrt{z^2 - (a_0^2 - b_0^2)}}{a_0 + b_0}, \quad \mu = \frac{a_1 + b_1}{a_0 + b_0}.$$

For our numerical implementation, we choose $a_0 = 7$, $b_0 = 5$, $a_1 = 5$, and $b_1 = 1$. Tables 5 and 6 show our results and Amano's results [2], respectively.

$n = m$	E_A	E_M
16	3.8(−03)	2.8(−02)
32	7.0(−04)	3.2(−03)
64	2.7(−05)	8.4(−05)

Table 6: Error norm (elliptic frame) using Amano's method

5. Conclusion

A boundary integral equation method was proposed for the numerical conformal mapping of doubly connected regions onto an annulus. Due to the presence of μ, the discretized integral equation leads to a system of nonlinear equations which are solved using optimization method. The advantage of this method is that it calculates the boundary correspondence functions and the inner radius simultaneously. Several mappings of the test regions were computed numerically using the proposed method. The numerical examples illustrate that the present method yields approximations of high accuracy for mappings of the test regions with smooth boundary.

References

[1] H.M. Antia, *Numerical Methods for Scientists and Engineers,* Tata McGraw-Hill Publishing Company Limited, New Delhi (1991).

[2] K. Amano, A Charge simulation method for the numerical conformal mapping of interior, exterior and doubly connected domains, *J. Comp. Appl. Math.,* **53** (1994), 353-370.

[3] K.E. Atkinson, *A Survey of Numerical Methods for the Solution of Fredholm Integral Equations,* Society for Industry and Applied Mathematics, Philadephia (1976).

[4] P. Henrici, *Applied and Computational Complex Analysis,* **3**, John Wiley, New York (1974).

[5] N. Kerzman, M.R. Trummer, Numerical conformal mapping via the Szegö kernel, *J. Comp. Appl. Math.,* **14** (1986), 111-123.

[6] P.K. Kythe, *Computational Conformal Mapping,* Birkhäuser-Boston, New Orleans (1998).

[7] W. Murray, *Numerical Methods for Unconstrained Optimization,* Academic Press, London and New York (1972).

[8] A.H.M. Murid, M.R.M. Razali, An integral equation method for conformal mapping of doubly-connected regions, *Matematika,* **15**, No. 2 (2000), 79-93.

[9] E.B. Saff, A.D. Snider, *Fundamentals of Complex Analysis,* Pearson Education, Inc., New Jersey (2003).

[10] G.T. Symm, Conformal mapping of doubly connected domain, *Numer. Math.,* **13** (1969), 448-457.

[11] L.N. Trefethen, *Numerical Conformal Mapping,* North Holland, Amsterdam (1986).

[12] R. Wegmann, *Methods for Numerical Conformal Mapping, In: Handbook of Complex Analysis: Geometric Function Theory* (Ed. R. Kühnau), **2**, Elsevier, Amsterdam (2005), 351-477.

[13] M.A. Wolfe, *Numerical Methods for Unconstrained Optimization,* Van Nostrand Reinhold Company, New York (1978).

[14] S. Wolfram, *Mathematica: A System of Doing Mathematics by Computer,* Addison-Wesley, Redwood City (1991).

[15] C. Woodford, *Solving Linear and Non-Linear Equations,* McGraw-Hill, New York (1992).